Carnegie Observatories Astrophysics Series, Vol. 1:
Coevolution of Black Holes and Galaxies, 2004
ed. L. C. Ho (Pasadena: Carnegie Observatories,
http://www.ociw.edu/ociw/symposia/series/symposium1/proceedings.html)

The Black Hole Masses of High-redshift Quasars

R. J. MCLURE[1] and M. J. JARVIS[2]
(1) Institute for Astronomy, Edinburgh University, Edinburgh EH9 3HJ, UK
(2) Sterrewacht Leiden, Postbus 9513, 2300 RA Leiden, The Netherlands

Abstract

A reliable method for estimating the black-hole masses of high-redshift quasars would provide crucial new information for understanding the nature and cosmological evolution of quasars. In this proceedings we summarize the results of our recent paper (McLure & Jarvis 2002) which provides a virial black-hole mass estimator based on rest-frame UV observables, thereby allowing reliable black-hole mass estimates to be obtained out to redshifts of $z \sim 2.5$ from optical spectra alone. All cosmological calculations assume $\Omega_m = 0.3, \Lambda = 0.7, H_0 = 70$ kms^{-1}Mpc^{-1}.

1.1 Introduction

The underlying assumption behind the virial black-hole mass estimate is that the motion of the broad-line emitting material in AGN is virialized. Under this assumption the width of the broad lines can be used to trace the Keplerian velocity of the broad-line gas, and thereby allow an estimate of the central black-hole mass via the formula $M_{\rm BH} = G^{-1}R_{\rm BLR}V_{\rm BLR}^2$, where $R_{\rm BLR}$ is the broad-line region (BLR) radius and $V_{\rm BLR}$ is the Keplerian velocity of the BLR gas. Currently, the most direct measurements of the central black-hole masses of powerful AGN are for 17 Seyferts and 17 PG quasars for which reverberation mapping has provided a direct measurement of $R_{\rm BLR}$; Wandel, Peterson, & Malkan (1999) and Kaspi et al. (2000) respectively.

An important result of these studies is the discovery of a correlation between $R_{\rm BLR}$ and the monochromatic AGN continuum luminosity at 5100Å (eg. $R_{\rm BLR} \propto \lambda L_{5100}^{0.7}$; Kaspi et al. 2000). By combining this luminosity based $R_{\rm BLR}$ estimate with a measure of the BLR velocity based on the FWHM of the Hβ emission line, it is now possible to produce a virial black-hole mass estimate from a single spectrum covering Hβ. This technique has recently been widely employed to investigate how the masses of quasar black holes relate to the properties of the surrounding host galaxies (eg. McLure & Dunlop 2001, 2002; Laor 2001) and the radio luminosity of the central engine (Dunlop et al. 2003; Lacy et al. 2001).

However, because the Hβ emission line is redshifted into the near-infrared at a redshift of $z \sim 1$, it is observationally expensive to use Hβ to estimate the black-hole masses of $z > 1$ quasars, with the vast majority of current studies concentrating on samples at $z \leq 0.3$. In this proceedings we summarize the evidence presented in McLure & Jarvis (2002) which suggests that the combination of 3000Å continuum luminosity and Mg II FWHM

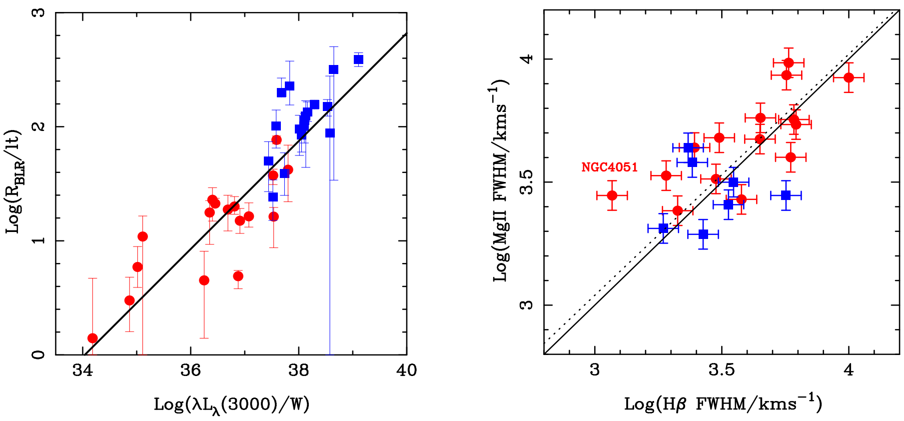

Fig. 1.1. The correlation between broad-line radius and AGN continuum luminosity at 3000Å. The 17 PG quasars are shown as squares and the 17 Seyfert galaxies are shown as circles. The best-fitting BCES bisector fit is shown as the solid line, and corresponds to $R_{\rm BLR} \propto \lambda L_{3000}^{0.47}$. Fig. 1.1b. A Log-Log plot of Mg II FWHM versus Hβ FWHM for the 22 objects from the RM sample for which it was possible to obtain measurements of both line-widths. The solid line is an exact 1:1 relation. The dotted line is the BCES bisector fit (Akritas & Bershady 1996), excluding NGC 4051, and has slope of 1.02 ± 0.14. NGC 4051 is a well known example of a narrow-line Seyfert galaxy.

can provide a reliable UV virial mass estimator in the redshift range $0.3 < z < 2.5$ from straightforward optical spectroscopy.

1.2 The Radius-Luminosity Relation

Fig. 1.1a. shows our analysis of the $R_{\rm BLR} - \lambda L_\lambda$ relation at 3000Å using a combined sample of 34 quasars and Seyfert galaxies with reverberation mapping measurements of $R_{\rm BLR}$ (RM sample, Kapsi et al. 2000; Wandel et al. 1999). The UV luminosities of the quasars are calculated from the data of Neugebauer et al. (1987), while the UV luminosities for the Seyfert galaxies are derived from our analysis of archival IUE spectra. The bisector fit is shown as the solid line in Fig. 1.1a, and is equivalent to:

$$R_{\rm BLR} = (25.2 \pm 3.0)\left[\lambda L_{3000}/10^{37} W\right]^{(0.47\pm0.05)}$$

where $R_{\rm BLR}$ is in units of light-days. We note here that the slope of the $R_{\rm BLR} - \lambda L_{3000}$ relation (0.47 ± 0.05) is entirely consistent with that expected for a constant ionization parameter (0.5). Furthermore, the scatter around the $R_{\rm BLR} - \lambda L_{3000}$ relation is smaller than that associated with the established relation based on 5100Å luminosity (see McLure & Jarvis (2002) for details).

1.3 Estimating the BLR Velocity

The main reason for adopting Mg II as the UV tracer of BLR velocity is that, like Hβ, MgII is a low-ionization line. Furthermore, due to the similarity of their ionization potentials, it is reasonable to expect that the MgII and Hβ emission lines are produced by gas at virtually the same radius from the central ionizing source. This assumption is directly

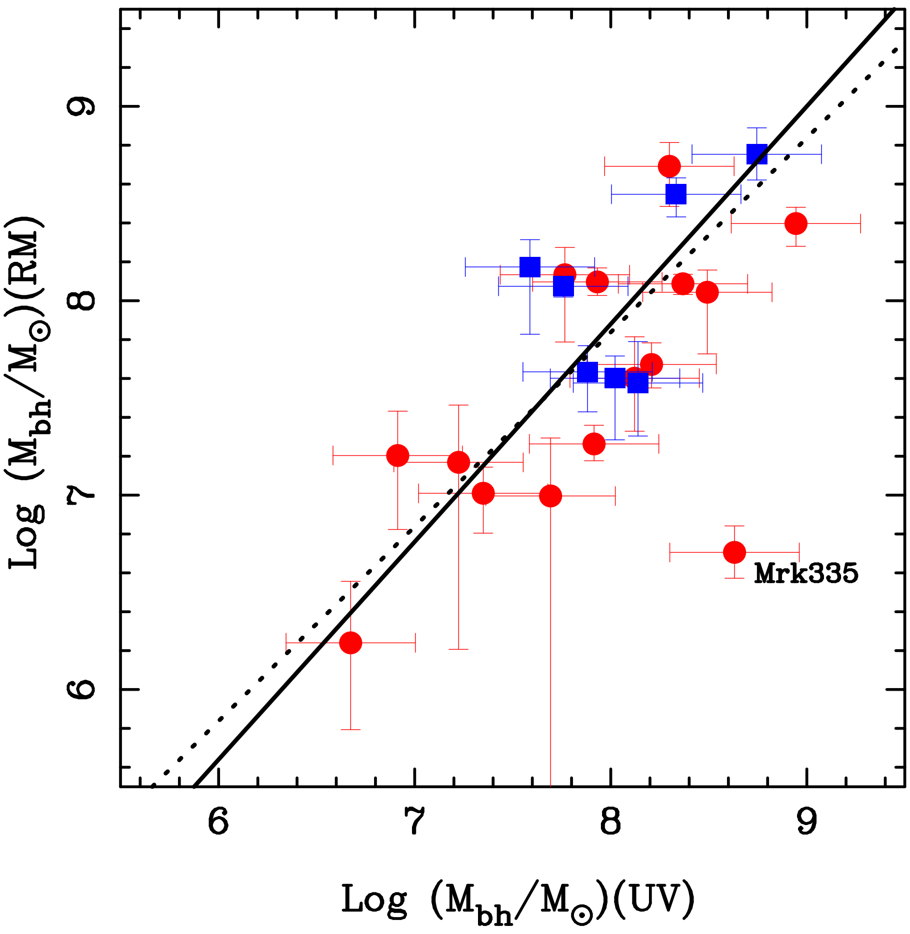

Fig. 1.2. Full reverberation mapping black-hole mass estimate (based on $R_{\rm BLR}$ measurements and the rms Hβ FWHM) plotted against the UV mass estimate (based on the $R_{\rm BLR}-\lambda L_{3000}$ relation of Fig. 1.1a. and the FWHM of MgII). The solid line is the BCES bisector fit, excluding Mrk 335 a narrow-line Seyfert, and has a slope of 1.12 ± 0.22. The dotted line is the adopted linear relation. Symbols as in Fig. 1.1.

tested in Fig. 1.1b. which shows a plot of Mg II FWHM versus Hβ FWHM for the 22 objects with reverberation mapping results (RM sample) for which it was possible to obtain Mg II FWHM measurements. Fig. 1.1b confirms that the FWHM of Mg II and Hβ do follow a 1:1 relation. This has two important consequences. Firstly, it allows us to directly adopt the $R_{\rm BLR}$ estimates from the correlation between $R_{\rm BLR}$ and 3000Å continuum luminosity. Secondly, because the line-widths of Mg II and Hβ should trace the same BLR velocities, we are able to simply substitute the FWHM of Mg II for that of Hβ in the virial mass estimator

1.4 The UV Black Hole Mass Estimator

Having determined the $R_{\rm BLR}-\lambda L_{3000}$ relation and the 1:1 scaling between Hβ FWHM and Mg II FWHM, we are now in a position to derive our UV black-hole mass esti-

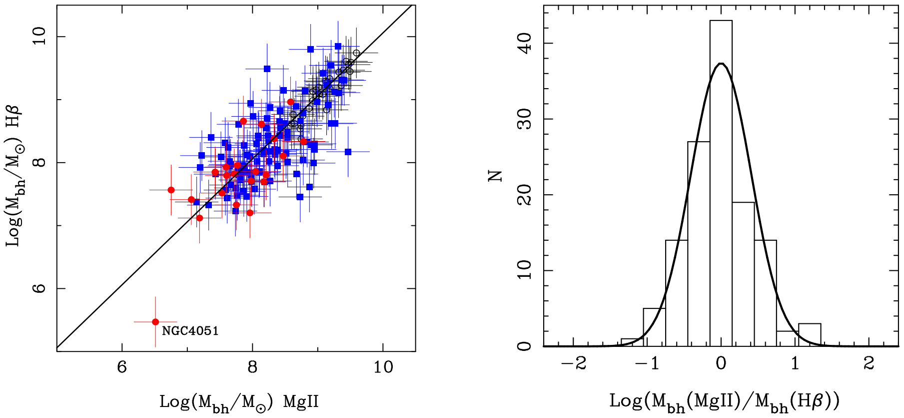

Fig. 1.3. The optical (Hβ) versus UV (MgII) virial black-hole estimators for 150 objects from the RM (filled circles), LBQS (filled squares) and MQS (open circles) samples. The solid line is the BCES bisector fit to the 128 objects from the MQS and LBQS samples and has a slope of 1.00 ± 0.08. The outlying NLS NGC4051 has been highlighted. Fig. 1.3b Histogram of $\log M_{\rm BH}(Mg\ II) - \log M_{\rm BH}(H\beta)$ for the 128 objects from the LBQS and MQS shown in Fig. 1.3a. Also shown is the best-fitting gaussian which has $\sigma = 0.41$.

mator. In Fig. 1.2 we show the reverberation mapping black-hole mass estimate versus the new UV mass estimate, which uses the $R_{\rm BLR} - \lambda L_{3000}$ relation to estimate $R_{\rm BLR}$ and the MgII FWHM to trace the BLR velocity. The solid line in Fig. 1.2 is the bisector fit to the data, excluding Mrk 335, and has the form: $\log M_{\rm BH}(RM) \propto 1.12(\pm 0.22) \log M_{\rm BH}(UV)$, consistent with a linear relation. In light of this, the dashed line in Fig. 1.2 shows the best-fitting linear relation which is adopted as our final calibration of the UV virial mass estimator. In terms of a useful formula the final calibration of the UV black-hole mass estimator is therefore:

$$\frac{M_{\rm BH}}{\rm M_{\odot}} = 3.37 \left(\frac{\lambda L_{3000}}{10^{37}\rm W}\right)^{0.47} \left(\frac{FWHM(Mg\ II)}{\rm kms^{-1}}\right)^{2}$$

Excluding Mrk 335, the mean difference between the reverberation and the UV estimator is : $< \log(M_{\rm BH})(RM) - \log(M_{\rm BH})(UV) >= 0.00 \pm 0.40\ (1\sigma)$. Provided the RM sample is representative of broad-line AGN, we conclude that the UV black-hole estimator can reproduce the reverberation black-hole mass to within a factor of 2.5 (1σ).

1.5 Application to the MQS and LBQS

In Fig. 1.3. we show the optical black-hole mass estimator plotted against the new UV black-hole mass estimator for a combined sample of 150 objects, comprising 99 from the Large Bright Quasar Survey (Forster et al. 2001), 29 from the radio-selected Molonglo Quasar Sample (Baker et al. 1999) and the 22 objects of the RM sample. Also shown is the BCES bisector fit to the LBQS and MQS objects which has the form:

$$\log M_{\rm BH}(H\beta) = 1.00(\pm 0.08) \log M_{\rm BH}(Mg\ II) + 0.06(\pm 0.67)$$

which, as expected, is perfectly consistent with a linear relation. In Fig. 1.3b we show a histogram of $\log M_{\rm BH}(Mg\ II) - \log M_{\rm BH}(H\beta)$ for the 128 objects from the LBQS and MQS.

The solid line shows the best-fitting gaussian which has $\sigma = 0.41$. These results lead us to conclude that, compared to the traditional optical black-hole mass estimator, the new UV estimator provides results which are unbiased and of equal accuracy.

1.6 Conclusions

The main conclusions of this study can be summarized as follows:

- The correlation between $R_{\rm BLR}$ and 3000Å continuum luminosity is found to display less scatter than the established correlation with 5100Å luminosity, and to be consistent with the $R_{\rm BLR} \propto \lambda L_{\lambda}^{0.5}$ relation expected for a constant ionization parameter.
- Combining the $R_{\rm BLR} - \lambda L_{3000}^{0.47}$ relation with the FWHM of Mg II produces a virial black-hole mass estimator based on rest-frame UV observables which is capable of reproducing black-hole masses determined from reverberation mapping to within a factor of 2.5 (1σ)
- An application to objects from the LBQS & MQS demonstrates that the new UV black-hole mass estimator produces results which are unbiased, and of equal accuracy to the established optical (Hβ) black-hole mass estimator.

References

Akritas M. G., & Bershady M. A. 1996, ApJ, 470, 706
Baker J. C., Hunstead R. W., Kapahi V. K., & Subrahmanya C. R. 1999, ApJS, 122, 29
Dunlop J. S., McLure R. J., Kukula M. J., Baum S. A., O'Dea C. P., & Hughes D. H. 2003, MNRAS, 340, 1095
Forster K., Green P. J., Aldcroft T. L., Vestergaard M., Foltz C. B., & Hewett P. C. 2001, ApJS, 134, 35
Lacy M., Laurent-Muehleisen S. A., Ridgway S. E., Becker R. H., & White R. L. 2001, ApJ, 551, L17
Laor A. 2001, ApJ, 553, 677
McLure R. J., & Dunlop J. S. 2001, MNRAS, 327, 199
McLure R. J., & Dunlop J. S. 2002, MNRAS, 331, 795
McLure R. J., & Jarvis M. J. 2002, MNRAS, 337, 109
Neugebauer G., Green R. F., Matthews K., Schmidt M., Soifer B. T., & Bennett J. 1987, ApJS, 63, 615
Wandel A., Peterson B. M., & Malkan M. A. 1999, ApJ, 526, 579